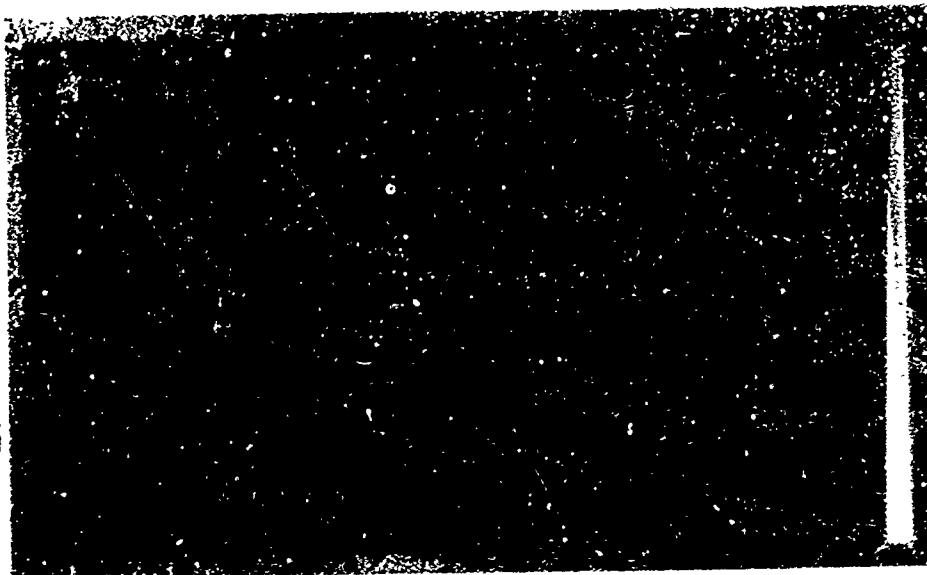


AD703247



DISTRIBUTION OF THIS DOCUMENT IS UNLIMITED

# Project THEMIS

CONTRACT ONR-N00014-68-A-0152

University of Notre Dame  
college of engineering  
notre dame, indiana

46556

Reproduced by the  
CLEARINGHOUSE  
for Federal Scientific & Technical  
Information Springfield Va. 22151

MAGNETOSTRICTION AND MAGNETIC ANISOTROPY  
IN SOME IRON RICH  
IRON-COBALT-ALUMINUM ALLOYS

by

M. Kuruzar, M. Phadke  
and  
A. E. Miller

February, 1970

Document cleared for public release and sale:  
Its distribution is unlimited.

Project THEMIS  
UNIVERSITY OF NOTRE DAME  
College of Engineering  
Notre Dame, Indiana 46556

Contract  
N00014-68-A-0152 (NR 260-112/7-13-67)  
Office of Naval Research

TECHNICAL REPORT  
NUMBER:  
THEMIS-UND-70-6

## FOREWORD

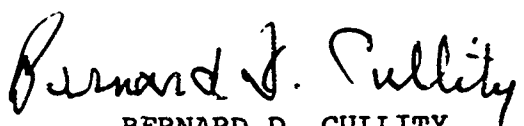
This technical report was prepared by the Magneto-mechanical Systems Group under Project THEMIS at the University of Notre Dame, College of Engineering.

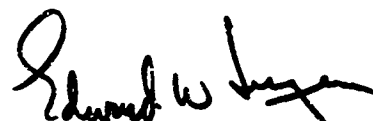
The research was performed under the sponsorship of the Department of the Navy, Office of Naval Research, Washington, D. C. 20360, with funding under Contract N00014-68-A-0152 and In-House Account Number UND-99850. The contract is under the technical guidance of Commander Herman D. Winfree, USN, Director of Undersea Programs (Code 466) of the Office of Naval Research.

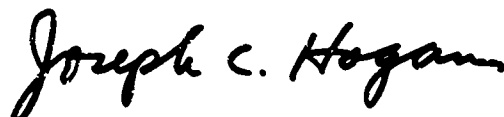
The authors wish to express their appreciation to Mrs. Evelyn Friedman for her typing of the manuscript and to Professor Hugh P. Ackert for the preparation of the illustrations.

Readers are advised that reproduction in whole or in part is permitted for any purpose of the United States Government.

This technical report has been reviewed and approved for submittal to the sponsoring agency on February 25, 1970.

  
BERNARD D. CULLITY  
Group Leader  
Magnetomechanical Systems

  
EDWARD W. JERGER  
Program Manager  
Project THEMIS

  
JOSEPH C. HOGAN  
Dean, College of Engineering  
University of Notre Dame

## ABSTRACT

The magnetic anisotropy and magnetostriction of single crystals and the magnetostriction of some polycrystalline specimens of several Fe rich Fe-Co-Al alloys has been experimentally determined. Specialized apparatus and procedures for alloy preparation, single crystal growth, crystal cutting, crystal orientation, magnetization and magnetostriction studies have been developed.

The first anisotropy constants,  $K_1$ , for 75Fe-15Co-10Al (wt.%), 85Fe-10Co-5Al, 80Fe-10Co-10Al and 80Fe-15Co-5Al alloys were found to be 79,000, 2,000, 282,000, and 39,000 (ergs/cc), respectively; the  $\lambda_{100}$  values were found to be  $+3.5 \times 10^{-6}$ ,  $+10.6 \times 10^{-6}$ ,  $+19.4 \times 10^{-6}$ , and  $+17.5 \times 10^{-6}$ , respectively; and the  $\lambda_{111}$  values were found to be  $+6.2 \times 10^{-6}$ ,  $-5.6 \times 10^{-6}$ ,  $+9.5 \times 10^{-6}$ , and  $-4.9 \times 10^{-6}$ , respectively.

## TABLE OF CONTENTS

Chapter	Page
I. INTRODUCTION	1
1-1 General	1
1-2 Metallurgical Parameters to be Considered	3
1-3 Selecting an Alloy System	7
II. EXPERIMENTAL PROCEDURE	8
2-1 Materials	8
2-2 Preparation of Polycrystalline Samples	8
2-3 Preparation of Single Crystal Samples	10
2-4 X-Ray and Metallographic Methods	12
2-5 Magnetic Measurements	13
III. RESULTS	15
3-1 X-Ray Studies	15
3-2 Texture Studies	17
3-3 Magnetostriction Studies	18
3-4 Magnetization Studies	28
IV. CONCLUSIONS	30

## LIST OF FIGURES

Figure		Page
1.1	A magnetostrictive transducer as an energy conversion device	4
1.2	Saturation magnetostriction in the [100] and [111] crystallographic directions of cobalt and aluminum alloys with iron	7a
1.3	Magnetic anisotropy in cobalt and aluminum alloys with iron	7b
2.1	Diagram of the arc melter used for preparation of Fe-Co-Al alloys	8a
2.2	Diagram of the vacuum furnace used for growth of Fe-Co-Al alloy single crystals	11
2.3	Schematic of system used to measure magnetostriction	14
2.4	Schematic of a vibrating-sample magnetometer	16
3.1	Magnetostriction in cast and formed 85Fe-10Co-5Al alloys	19
3.2	Sketch illustrating the method used to obtain saturation magnetostriction	21
3.3	Saturation magnetostriction measured in the [100], [110], and [111] directions as a function of angle $\theta$ for the 75Fe-15Co-10Al alloy	24
3.4	Saturation magnetostriction measured in the [100], [110], and [111] directions as a function of angle $\theta$ for the 85Fe-10Co-10Al alloy	25
3.5	Saturation magnetostriction measured in the [100], [110], and [111] directions as a function of angle $\theta$ for the 80Fe-10Co-10Al alloy	26
3.6	Saturation magnetostriction measured in the [100], [110], and [111] directions as a function of angle $\theta$ for the 80Fe-15Co-5Al alloy	27

## I. INTRODUCTION

### 1-1 General

Magnetostriction is a term that is used to describe the dimensional changes of a ferromagnetic material when it is subjected to a magnetic field or, conversely, the change in the material's magnetic properties when its dimensions are altered by an externally applied stress. Devices, in which these materials are coupled to an alternating magnetic field, are of great technological importance since they form the basis for echo-sounding and nondestructive testing systems as well as ultrasonic cleaning, drilling and cutting units.

Although a detailed discussion of the basic phenomenon of ferromagnetism and magnetostriction is beyond the scope of this report and definitive works in the field [1], [2], and [3] should be consulted if a deeper understanding is desired, nevertheless, it is appropriate to elucidate briefly a couple of terms that are frequently used in this report.

1. Longitudinal Magnetostriction. A measure of a ferromagnetic materials sensitivity to the magnetostriction effect is the magnitude of the strain  $\lambda$  (defined as  $\Delta l/l$ , where  $l$  is the original length) experienced by the material in the direction of an applied magnetic field. Longitudinal magnetostrictive strain,  $\lambda$ , may be either positive or negative, indicating an expansion or a contraction in the direction of the magnetic field respectively.

2. Saturation Magnetostriction. The longitudinal magnetostrictive strain reaches a maximum, constant value at some value of applied magnetic field. This maximum in  $\lambda$  is called the saturated value,  $\lambda_s$ .
3. Magnetocrystalline Anisotropy. In a single crystal of a ferromagnetic material there is a preferred crystallographic direction along which the intrinsic magnetization lies. The energy, called anisotropy energy, required to turn the magnetization vector out of the preferred direction is indicated by a general anisotropy constant,  $K$ .

The ferrite ceramics [4], nickel and nickel base [5] alloys are in common use today as magnetostrictive transducer elements. These materials have  $\lambda_s$  values from  $30 \times 10^{-6}$  in/in to  $150 \times 10^{-6}$  in/in with the metallic phases occupying the lower end of the range. These materials face tough competition in the transducer field from ceramic piezoelectric materials which have electrostrictive strains three orders of magnitude larger than the  $\lambda_s$  of the magnetostrictive materials [6]. However, ceramic materials in general suffer from two serious shortcomings:

- 1) they are brittle and have a low resistance to impact loads, and
- 2) they have a high notch sensitivity and very poor fatigue resistance.

Hence, the metallic magnetostrictive materials offer definite advantages since they are vastly superior to ceramics in the above areas. They are, however, somewhat limited



in their application due to the fact that  $\lambda_s$  is usually not as large as required by the device application. The greatly superior reliability of a transducer device constructed with metallic active elements certainly merits an expenditure of effort to develop alloys with larger and more useful values of  $\lambda_s$ .

### 1-2 Metallurgical Parameters to be Considered

The development of metallic alloys for magnetostrictive transducer applications is a many faceted undertaking that requires the simultaneous optimization of several different but interdependent metallurgical variables; e.g., alloy content, texture, residual stress, etc. This type of optimization of variables is commonly encountered in engineering and at best is a very tedious task even in those situations where reasonably accurate theories exist from which the important parameters and their interrelations can be extracted. In the case of magnetostriction, where a complete understanding of the fundamental processes involved in the phenomenon is lacking, it is difficult to establish and optimize the controlling parameters for the most simple case, that of a pure metal, and it becomes extraordinarily difficult to predict the effects of alloying on these parameters. Hence, it becomes necessary to begin by studying a simple model from which 1) some of the controlling parameters can be more definitely established, 2) some simple interrelations between these parameters can be deduced; and 3) the course of the research program can be outlined.

If a magnetostrictive device, such as the one shown schematically in Figure 1.1, is considered as a unit with the primary function of converting electrical work into

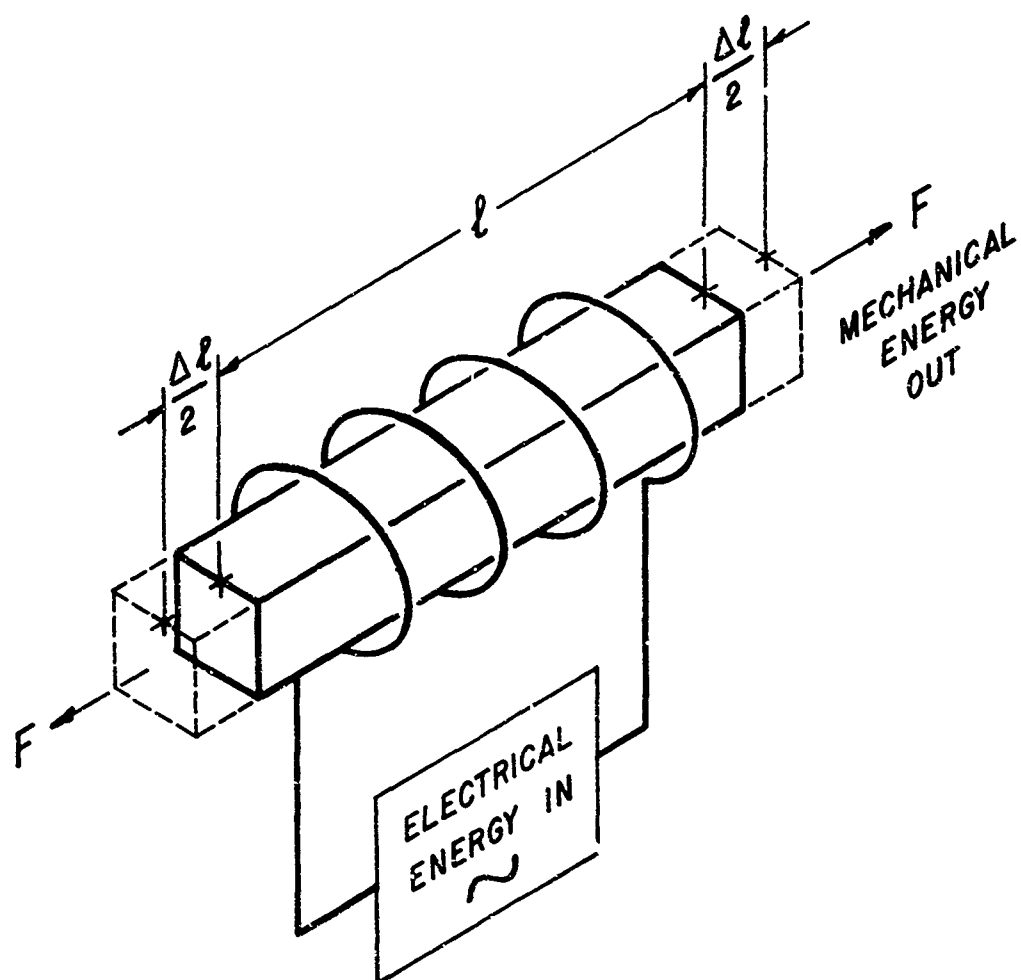


Figure 1.1 A Magnetostrictive Transducer  
as an Energy Conversion Device

mechanical work or vice versa, then good design principles dictate that 1) the mechanical work out of the system should be as large as possible and 2) the efficiency of the unit in converting electrical work into mechanical work should be a maximum. Assuming that a fictitious "magnetostrictive force",  $F$ , "produces" the change in length,  $\Delta l$ , of the magnetostrictive element with a zero field length,  $l$ , upon the application of an axial magnetic field, then the mechanical work done by the magnetostrictor is,

$$F \times \Delta l$$

and since  $E = F/A / \Delta l/l$  where  $E$  is the elastic modulus and  $A$  is the cross sectional area normal to the force,

$$\text{then} \quad \text{Work}_{\text{Mech}} = A l E \left( \frac{\Delta l}{l} \right)^2$$

$$\text{and} \quad \text{Work}_{\text{Mech}} / \text{Volume of Material} = E \left( \frac{\Delta l}{l} \right)^2 = E (\lambda)^2.$$

Now that the form of the output work has been established the electrical input work can be described as a sum of terms:

- 1) the work done against the "magnetostrictive force" =  $E(\lambda)^2$ ,
- 2) the work done against magnetocrystalline anisotropy =  $K$ ,
- 3) the work that is done to counteract the effect of internal residual stresses,  
 $\sigma_{R'} = \sigma_R \lambda$ ,
- 4) the work that must be done to overcome the demagnetizing effects arising from the presence of free magnetic poles as the result of voids, nonmagnetic inclusions or

microcracks =  $\bar{f}(\rho)$ , where  $f(\rho)$  indicates that the work required is a function of the number and distribution of the free magnetic poles.

Hence, the efficiency of the device in going from zero field to some static applied magnetic field is:

$$\text{Eff} = \frac{E(\lambda)^2}{E(\lambda)^2 + K + \sigma_R \lambda + f(\rho)}.$$

From the above expression for efficiency deduced on the basis of the simple model discussed it is now possible to focus attention on those metallurgical parameters that are of obvious importance. First, the term,  $\sigma_R \lambda$ , has a deleterious effect on the efficiency but can be eliminated by adopting rather standard metallurgical annealing practices used for internal stress relief. Second,  $f(\rho)$ , can also be reduced to a negligible value by using reasonable care in material preparation and in subsequent forming operations. Third, the anisotropy energy,  $K$ , is an intrinsic property of the material as are  $\lambda$  and  $E$ , all of which are a function of the composition of the material. Thus, it appears that the objectives of alloying to produce better transducer material characteristics should be to 1) maximize  $\lambda$  and  $E$  so that the magnitude of the mechanical work that the device can do is as large as possible and 2) minimize  $K$  so as to obtain the highest possible efficiency.

In the above analysis, only the static field situation was developed because of its simplicity and also since little is to be gained by complicating the model by introducing an oscillating magnetic field. However, the technologically important applications of magnetostrictive materials are to devices that operate in a cyclic manner and

produce vibratory mechanical work. This cyclic operation introduces at least two other losses that must be considered - hysteresis and eddy current losses. However, in general it is found that alloying to minimize  $K$  also increases permeability and decreases the size of the hysteresis loop. In order to reduce the eddy currents it would be desirable to alloy to increase resistance, which would in turn increase flux penetration and reduce hysteresis losses, but this is not usually profitable since in many cases the effects are not large and in those cases where they are serious complicating factors arise; e.g.,  $\lambda_s$  becomes very small, or extremely brittle, ordered phases exist. Similar complications are encountered if alloying is performed to maximize  $E$ . Thus, in the final analysis it can be said that the primary objectives of a program to develop better magnetostrictive metallic alloys should be to control alloy content so as to maximize  $\lambda_s$  and minimize  $K$ .

### 1-3 Selecting an Alloy System

A survey of the literature [7], [8], [9] concerning magnetostriction indicates that the addition of either aluminum or cobalt to iron increases the saturation magnetostriction,  $\lambda_s$ , in the [100] direction to values that are larger than the reported  $\lambda_s$  for nickel, Figure 1.2. It is interesting to speculate that the observed increase in  $\lambda_s$  produced by alloying the individual elements Al and Co with Fe could be additive in such a manner that an Fe-rich Fe-Co-Al alloy exists that has a  $\lambda_s$  larger than that displayed in either of the binary systems. However, as shown in Figure 1.3, the anisotropy constants for both Fe-Co and Fe-Al alloys are positive [7] thus making it rather unlikely that too much could be gained in this respect. But, since  $\lambda_s$  appears as a squared term it was felt that the possibility

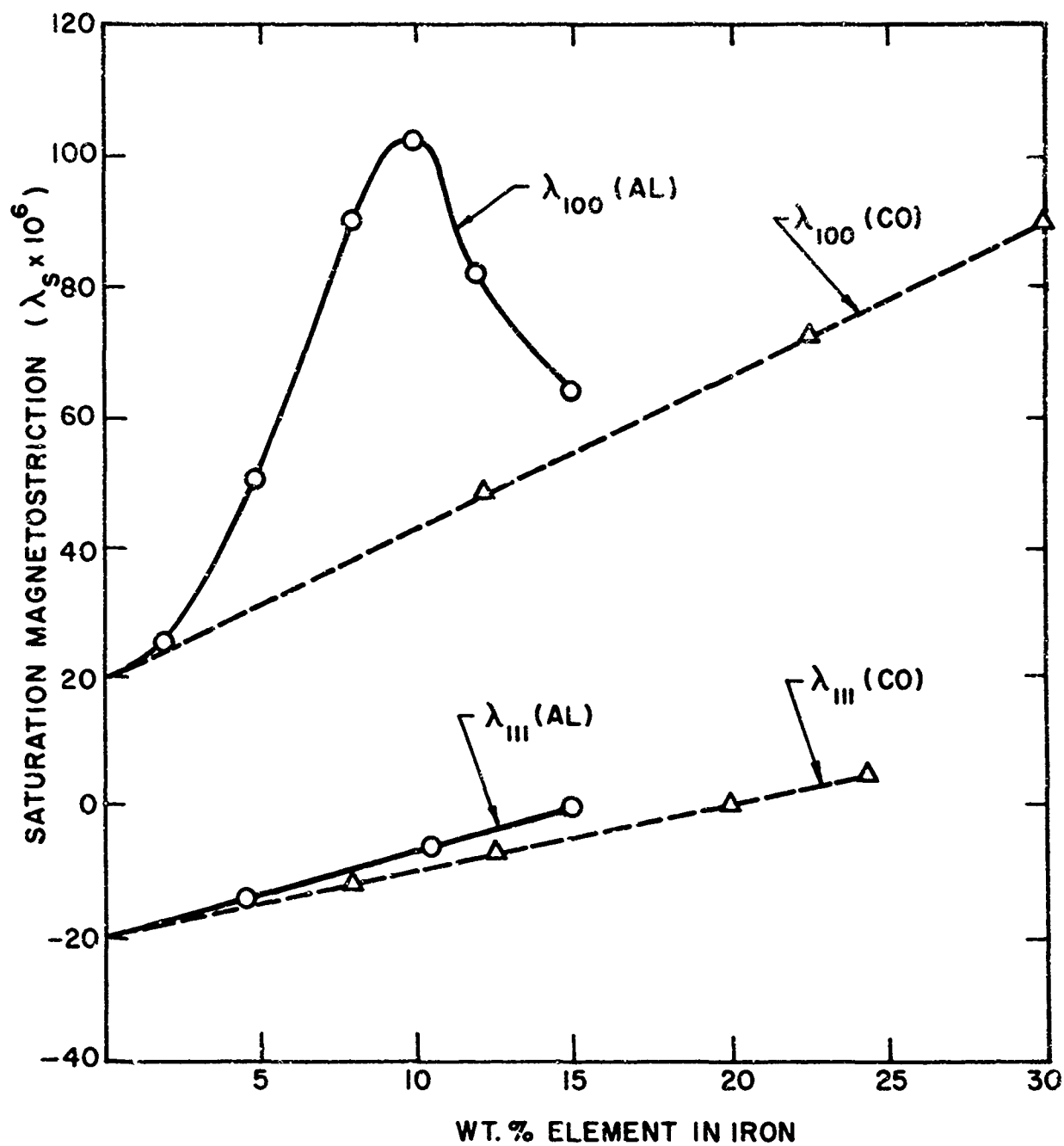


Figure 1.2 Saturation Magnetostriction in the [100] and [111] Crystallographic Directions of Cobalt and Aluminum Alloys with Iron

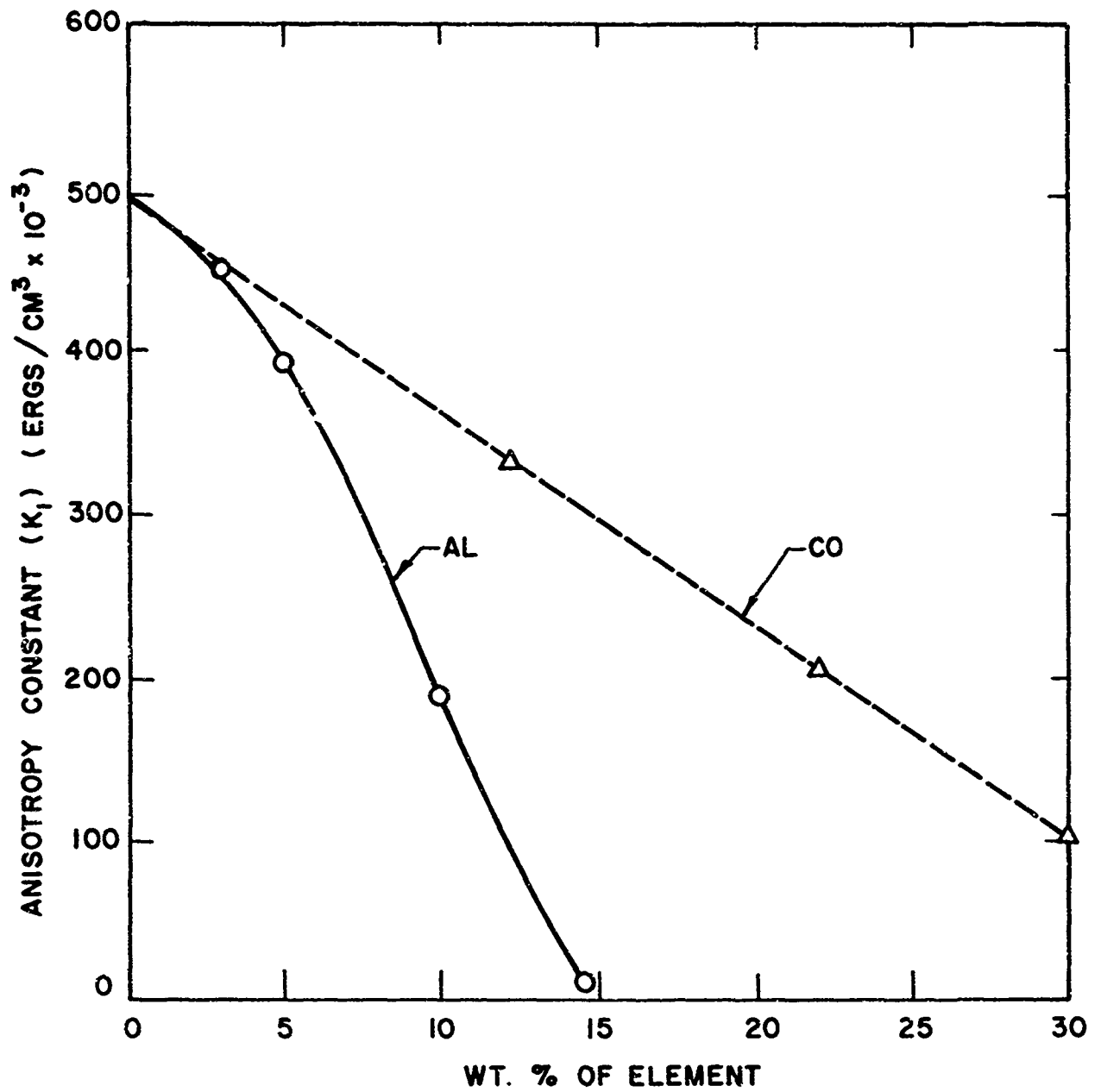


Figure 1.3 Magnetic Anisotropy in Cobalt and Aluminum Alloys with Iron

of increasing  $\lambda_f$  takes precedence and hence it was decided to study the solid solution alloys in the Fe-rich corner of the Fe-Co-Al system.

## II. EXPERIMENTAL PROCEDURE

### 2-1 Materials

The iron, cobalt and aluminum used in this study were obtained from Crucible Steel, United Mineral and Chemical Corp., and Aluminum Corporation of America, respectively. The major impurities in these materials are shown in Table 2.1.

Table 2.1 Major Impurities in Starting Materials in ppm

<u>Ferrovac E Iron</u>		<u>Aluminum</u>		<u>Cobalt</u>	
Ni	350	Cu	20	Ni	25
Si	<300	Fe	30		
Cu	<100	Si	20		
Cr	<100				
S	50				
C	40				
Al, P, Mn, Mg, Ca <30					

### 2-2 Preparation of Polycrystalline Samples

All of the alloys, single crystal and polycrystalline, used in this study were initially formed by arc melting weighed amounts of the constituents in a He atmosphere. To do this, it was necessary to design and construct the inert-atmosphere, nonconsumable tungsten electrode, arc-melting system diagrammed in Figure 2.1. This unit facilitates the production of 1 in. diameter by 1/4 in. thick, 30 gm. buttons



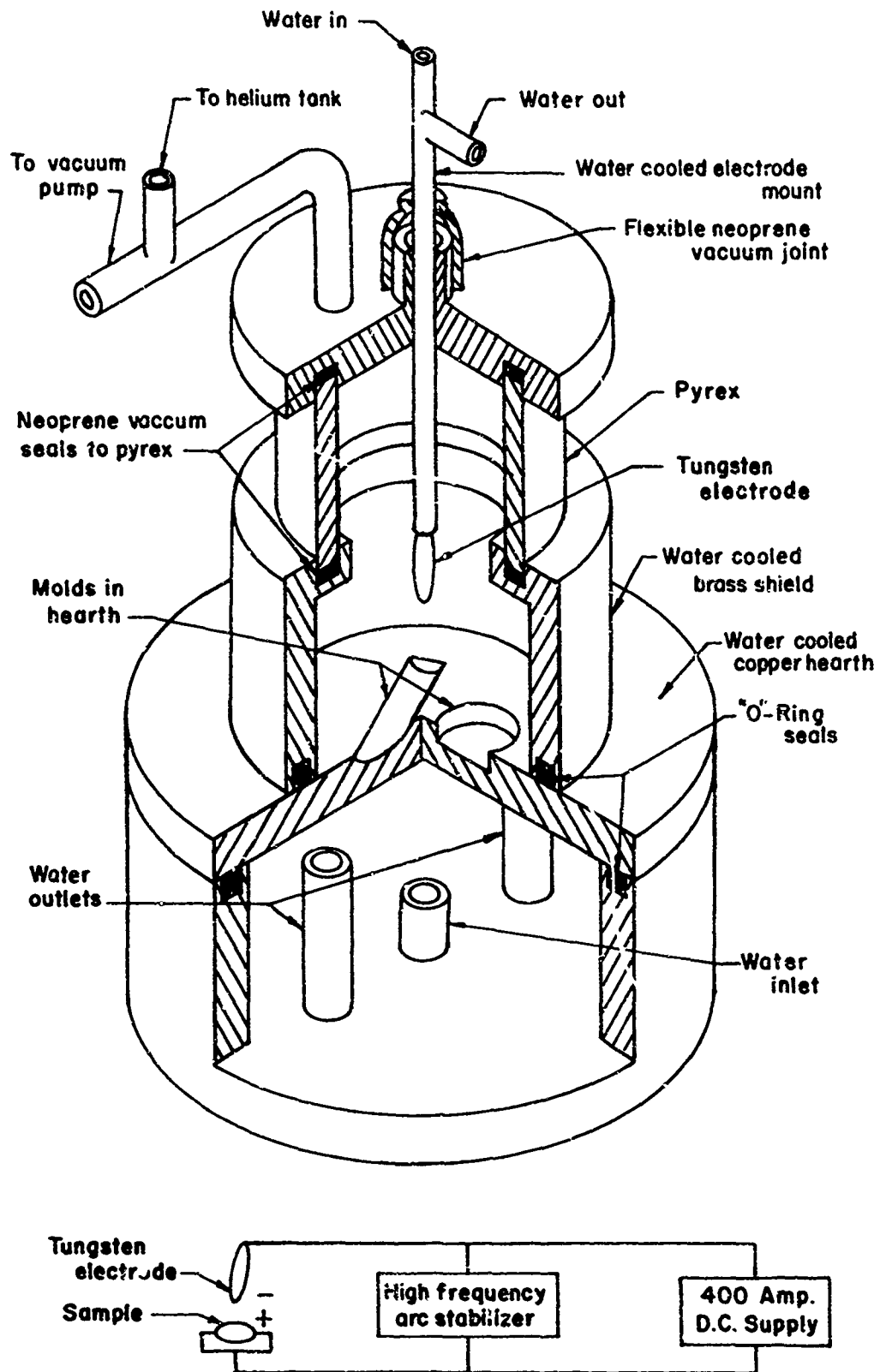


Figure 2.1 Diagram of the Arc-Melter used for preparation of Fe-Co-Al Alloys

and has a trough in the water cooled copper hearth for the formation of 1/4 in. x 1/4 in. x 3-1/4 in. billets.

The materials were degreased with acetone, pickled (Fe and Co in dilute sulfuric acid and Al in Tucker's etch) and dried before weighing. The constituents were placed in the circular depression in the copper hearth; the system was then evacuated to about 10 microns of Hg and back-filled with He gas. The arc was established between the sample and the water cooled tungsten electrode and "played" over the material until a molten pool was formed that contained all of the added material. In order to insure thorough mixing of the constituents the alloy "buttons" were turned and re-melted from the opposite side several times. The buttons were then transferred to the trough and melted into a rod shape. Weight losses due to vaporization during the alloy formation were negligible and the alloys were taken to have the initially calculated composition. Compositions of alloys prepared and studied in the program are listed in Table 2.2.

Table 2.2 Composition of Alloys Studied in wt. %

<u>Constituent</u>	<u>Fe</u>	<u>Co</u>	<u>Al</u>	<u>Sample Number</u>
	75	10	15	1
	75	15	10	2 *
	85	10	5	3 *
	75	20	5	4
	80	10	10	5 *
	80	15	5	6 *

\*Indicates compositions that were also prepared and studied in single crystal form.

In an attempt to break up the as-cast structures the

alloy billets were cut into rectangular parallelopipeds and subjected to alternate 1% reductions in thickness by cold rolling operations followed by 2 hr. anneals in argon at 610°C with subsequent furnace cool. This schedule was continued up to a total reduction in thickness of about 10% above which alloys 1, 2, 4, and 6 invariably developed large cracks. Alloys 3 and 5 were hot rolled in the 900-1100°C range where it was found that reductions in thickness of 40-60% could be readily obtained in only a few passes through the rolling mill.

### 2-3 Preparation of Single Crystal Samples

Single crystals of the ternary alloys noted in Table 2.2 were grown from the melt by the Bridgman technique. In the modification of this technique employed in this work a molten charge contained in a stabilized Zirconia crucible was lowered out of the hot zone. The bottom of the crucible was tapered and as the taper emerged from the hot zone a single seed nucleated at the point of the taper and this single seed continued to grow as the sample was extracted. Single crystals 3/8 in. in diameter and 2 in. long were produced with regularity at a withdrawal rate of 2 in./hr.

The vacuum furnace diagrammed in Figure 2.2 was constructed for the purpose of crystal growth. The heater element is a reactor grade graphite spiral 12 in. long with a bore of 1-1/2 in. With the tantalum radiation shields in place a uniform hot zone, 5°C maximum variance, about 4 in. long was obtained at 1500°C and  $1 \times 10^{-5}$  torr.

The charge was observed with an optical pyrometer through the viewing port on the top of the vacuum chamber. After the charge was observed to melt on heating, the sample

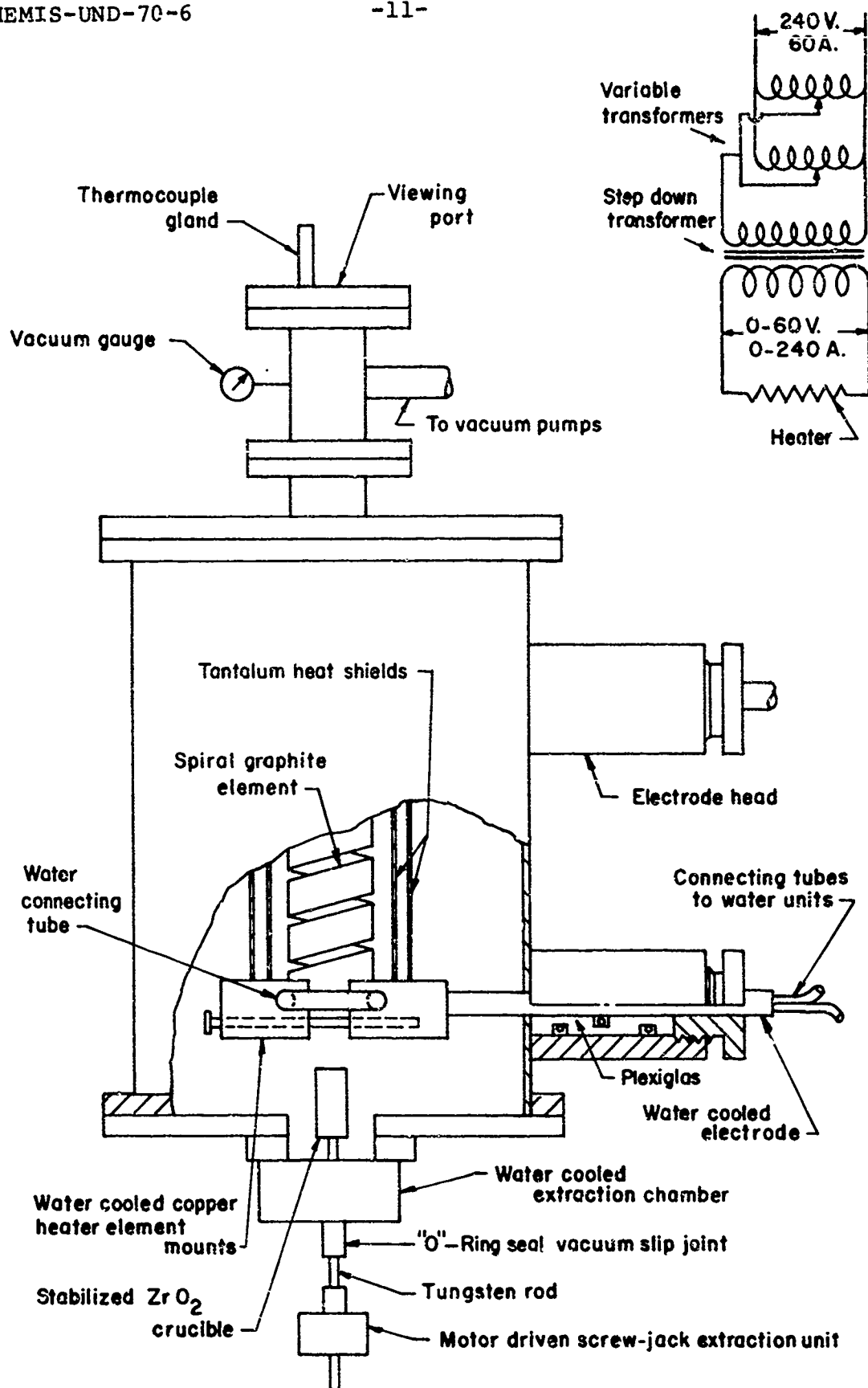


Figure 2.2 Diagram of the Vacuum Furnace used for Growth of Fe-Co-Al Alloy Single Crystals

higher than where the melting was first observed. After the sample had been extracted the furnace was slowly cooled.

The single crystal rods were aligned by an X-ray Laue technique and placed in a Servo-Met spark cutter. Single crystal discs about .020 in. thick and 3/8 in. in diameter were cut parallel to the {110} planes within about  $\pm 2^\circ$ . The discs were spark planed to obtain smooth and parallel surfaces, and annealed at 550°C for about 2 hours to relieve any possible strains induced by spark machining.

#### 2-4 X-Ray and Metallographic Methods

Standard powder X-ray diffraction techniques were used to verify the single phase, body-centered cubic nature of all the alloys studied. Powder for the analysis was obtained by filing the specimens with a hardened steel file. The powder was sealed in a glass capillary and exposed to Cr K<sub>α</sub> radiation. The sharpness of the resulting patterns indicated that it was unnecessary to anneal the powder before taking a pattern.

The crystallographic texture at various positions along the length of the polycrystalline samples was determined from integrated intensity measurements of the (200) and (110) diffraction lines using an X-ray diffractometer with a 1° incident slit and Cr K<sub>α</sub> radiation. The sample surfaces were first polished and then chemically milled with 2 pct. Nital to remove any possible cold work effects produced by polishing. The observed integrated intensity ratio of  $I_{(200)}/I_{(110)}$  was then compared to the predicted value of  $I_{(200)}/I_{(110)} = 1/5$  for a random orientation. This technique was used to follow the effect of various treatments on the texture of the specimens.

The back reflection Laue method was used to align all single crystals. The Laue spots obtained were sharp and singular indicating the lack of residual strains and low angle grains.

Standard metallographic procedures were used to prepare the alloys for microscopic examination. The alloys were etched using a 20 sec. dip in 50%  $H_2SO_4$  followed by a 10 sec. dip in 3% Nital.

#### 2-5 Magnetic Measurements

Magnetostriction studies of the polycrystalline samples were made with the set-up shown in Figure 2.3. SR-4 type strain gauges were attached to parallelepiped samples about  $1/4"$  x  $1/4"$  x  $3"$  in size. The sample was placed in a solenoid of known current-magnetic field characteristics with the long dimension along the axis of the solenoid. The solenoid current was changed in convenient increments and the resulting strain was measured on a BAM-1\* strain gauge bridge. After each strain measurement the DC supply to the solenoid was disconnected and the output of an AC variable transformer was connected. The AC voltage across the solenoid was then increased to a predetermined value and returned to zero. During this operation the sample was exposed to a steadily decreasing 60 hz magnetic field that served to demagnetize the specimen. After demagnetizing the specimen, the variable transformer was replaced by the DC power supply, the solenoid was energized to a predetermined level and the measurement procedure repeated.

---

\*Model BAM-1, Bridge Amplifier and Meter manufactured by Ellis Associates, Pelham, New York.

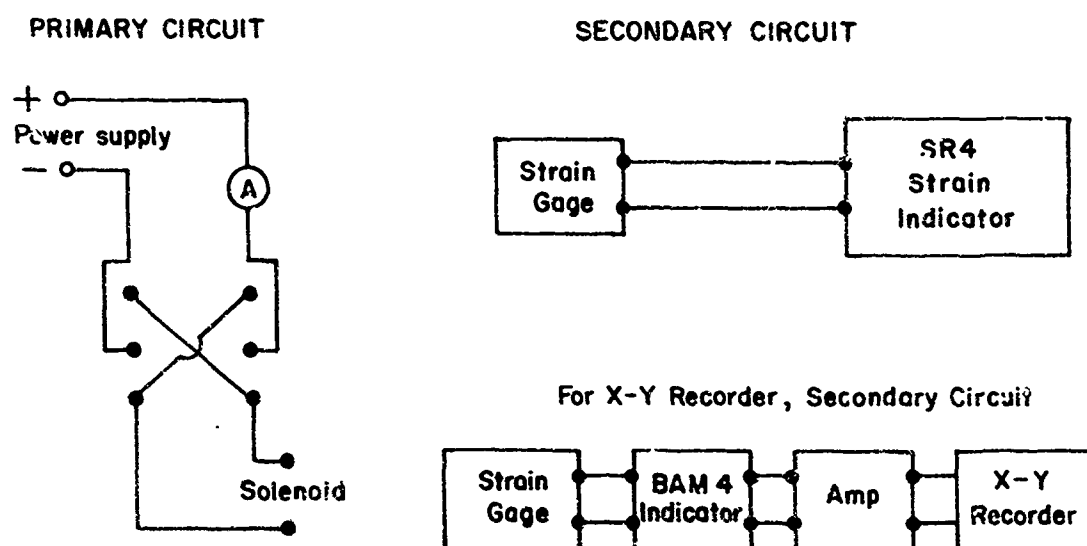


Figure 2.3 Schematic of System used to Measure Magnetostriction

A strain gauge technique similar to that described above, Figure 2.3, was used for the magnetostriction studies of the single crystals. Strain gauges were placed on the crystals in the [100], [111], and [110] crystallographic directions. Magnetostriction was plotted for each gauge direction for different field directions. The angle  $\theta$ , defined as the angle between the [100] crystallographic direction and the field direction, was varied from 0 to 180° in 10° increments.

The magnetic anisotropy was determined from magnetization vs. applied field curves automatically plotted for the [100], [111], and [110] crystallographic directions by a vibrating-sample magnetometer. The magnetometer constructed for this purpose is shown in Figure 2.4. In this technique the magnetized sample is vibrated at 102 hz perpendicular to the applied field. The time varying part of the oscillating dipole field is sensed by pick-up coils suitably placed in the vicinity of the sample. The output of the coils, calibrated against the saturation moment of nickel ( $54.55 \frac{\text{emu}}{\text{gm}}$ ), was amplified, rectified, and used to drive the y axis of a function plotter while the output of a Hall effect device placed in the magnet air gap was used to drive the applied field or x axis.

### III. RESULTS

#### 3.1 X-ray Studies

Metallographic and X-ray examination of the alloys studied showed that they were one phase solid solutions with an expanded alpha iron (body-centered cubic) structure, Table 3.1.



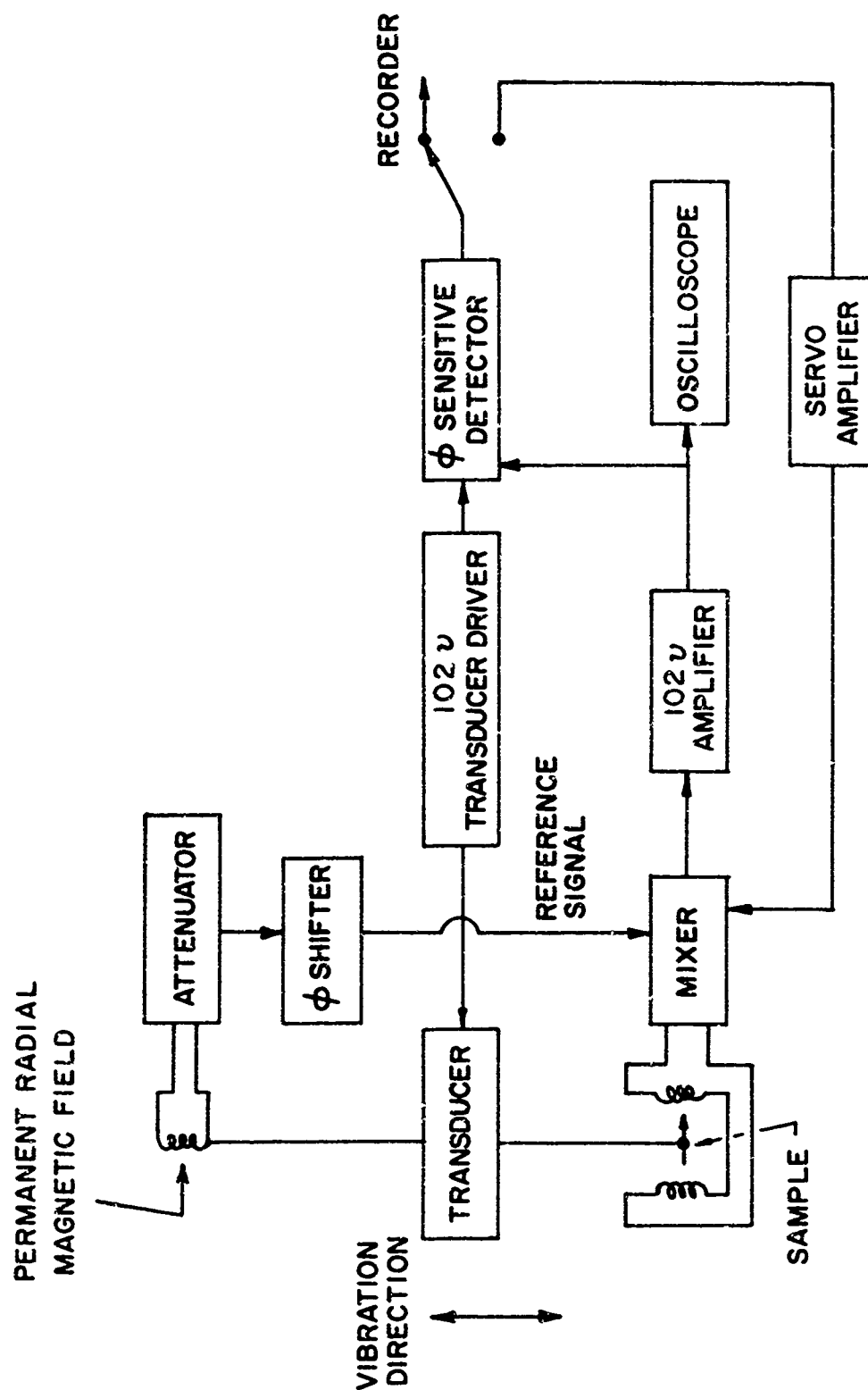


Figure 2.4 Schematic of a Vibrating-Sample Magnetometer

Table 3.1 Lattice parameters of single crystal alloys

Composition		$a_0$ , (Å)
wt.%	Fe-Co-Al	
	75-15-10	2.882
	85-10- 5	2.862
	80-10-10	2.890
	80-15- 5	2.878

### 3.2 Texture Studies

Many attempts were made to establish either a schedule of cold rolling and annealing processes or a hot rolling process that would break up the as-cast structure of the arc-melted samples and produce either a randomly oriented polycrystalline material or, more realistically, a material with uniform texture.

However, all such attempts were unsuccessful. This observation is not really too surprising when the following variables involved in the solidification of the arc-melted sample are considered:

- 1) Texture studies indicated that in general solidification took place with the (110) planes parallel to the copper hearth on the sides that the melt contacted the hearth. On the top side of the sample, however, a very uneven texture was observed.
- 2) The degree of (110) solidification texture appeared to depend upon:
  - a) degree of superheat,
  - b) rate at which the arc was moved along the length of the melt, and

- c) the manner in which the arc was extinguished when melting was complete.

These variables were difficult to control and hence despite all efforts polycrystalline samples with uniform texture along the sample length were not obtained.

### 3.3 Magnetostriction Studies

Even though samples of uniform texture could not be obtained it was none the less instructive to look at the magnetostriction of one of the more workable alloys. Figure 3.1 summarizes the results obtained for several 85Fe-10Co-5Al alloys that had been subjected to different mechanical working and heat treating processes. Although some of the alloys were hot worked at temperatures from 900 to 1100°C with reductions in thickness from 30 to 60% while others were cold worked by various amounts up to 20% followed by annealing at 800°C, the magnetostriction data lies within the band indicated. The fact that the band lies very close to the  $\lambda$  vs.  $H$  relation observed for Fe in the [110] direction indicates that the alloys probably have a strong [110] texture along the axis of the sample parallel to the magnetic field.

Experimentally it is found that the saturation magnetostriction measured on single crystals fits the two constant expression:

$$\lambda_s = h_1 (\alpha_1^2 \beta_1^2 + \alpha_1^2 \beta_1^2 + \alpha_1^2 \beta_1^2 - 1/3) \\ + 2h_2 (\alpha_1 \alpha_2 \beta_1 \beta_2 + \alpha_2 \alpha_3 \beta_2 \beta_3 + \alpha_3 \alpha_1 \beta_3 \beta_1)$$

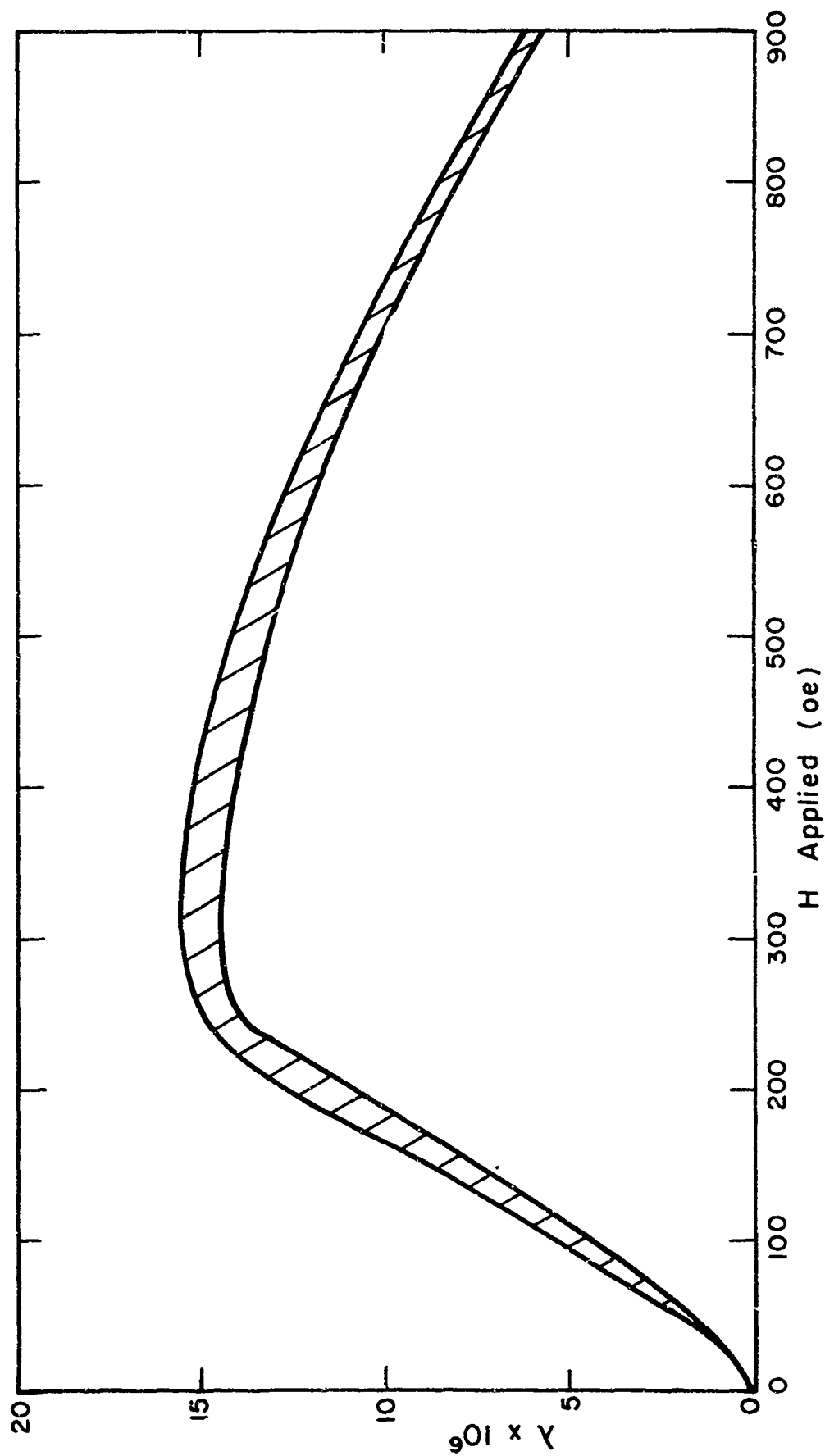


Figure 3.1 Magnetostriction in Cast and Formed 85Fe-10Co-5Al Alloys

where  $\lambda_s$  is the saturation magnetostriction measured in the crystallographic direction having direction cosines of  $\beta_1$ ,  $\beta_2$ , and  $\beta_3$  with the crystal axis when the crystal is magnetized in a direction having direction cosines of  $\alpha_1$ ,  $\alpha_2$ , and  $\alpha_3$  with respect to the same crystallographic axis. The magnetostriction constants  $h_1$  and  $h_2$  are related to the directional and polycrystalline saturation magnetostriction values:

$$\lambda_{100} = \frac{2}{3} h_1$$

$$\lambda_{111} = \frac{2}{3} h_2$$

$$\lambda_{110} = \frac{1}{6} h_1 + \frac{1}{2} h_2$$

$$\lambda_p = \frac{4}{15} h_1 + \frac{2}{5} h_2$$

where  $\lambda_{100}$ ,  $\lambda_{111}$ , and  $\lambda_{110}$  are the values in the respective directions and  $\lambda_p$  is the value for polycrystalline material with a random grain orientation.

The data was analyzed in a manner similar to that described by Hall [7]. The values of saturation magnetostriction were obtained by extrapolating the magnetostriction versus field strength curves to zero field strength, Figure 3.2. The extrapolated value of magnetostriction at zero field was taken to be the saturation magnetostriction and was used in all further calculations.

There are two experimental situations that simplify the determination of the magnetostriction constants,  $h_1$  and  $h_2$ :

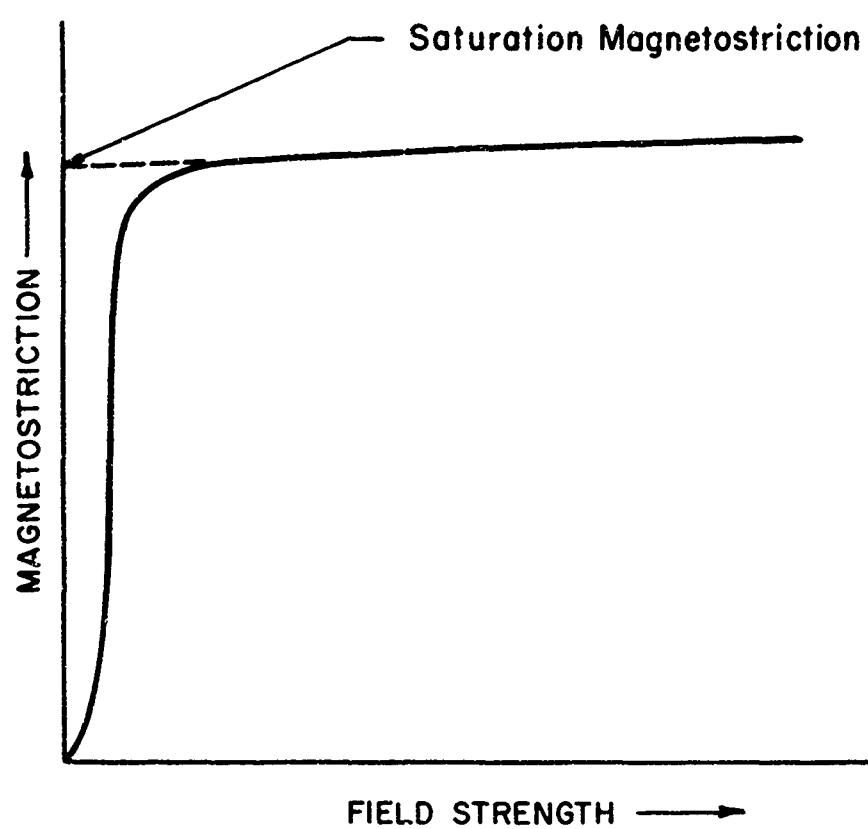


Figure 3.2 Sketch Illustrating the Method used to Obtain Saturation Magnetostriiction

- 1) With the strain gauge mounted on a crystal whose surface is parallel to the {110} planes and the gauge placed so as to measure strain in the {100} direction, the angular coefficient of the  $h_2$  term is zero. Thus a mean value of  $h_1$  can be determined from:

$$h_1 = \frac{\sum \lambda \text{ (gauges parallel to [100], } \theta = 0 \text{ to } 180)}{\sum (h_1 \text{ coefficients, } \theta = 0 \text{ to } 180)}$$

- 2) With the strain gauge mounted on a crystal surface parallel to {110} planes and placed so as to measure strain in the [111] direction, the angular coefficient of the  $h_1$  term is zero. Thus a mean value of  $h_2$  can be determined from:

$$2h_2 = \frac{\sum \lambda \text{ (gauge parallel to [111], } \theta = 0 \text{ to } 180)}{\sum (h_2 \text{ angular coefficients, } \theta = 0 \text{ to } 180)}$$

The saturation magnetostriction values obtained as a function of  $\theta$  for the various alloys in the [100], [110], and [111] directions are shown in Figures 3.3 - 3.6. The data obtained for the saturation magnetostriction for the [100] and [111] directions were used to determine the magnetostriction constants  $h_1$  and  $h_2$  as described above. The results are shown in Table 3.2.

The shape of the sample has a small effect on the measured magnetostriction and slight corrections to  $h_1$  and  $h_2$  are usually required. The corrections are given as:

Table 3.2  
Saturation magnetostriction values and magnetostriction constants

Composition wt. % Fe-Co-Al	$h_1 \times 10^6$	$h_2 \times 10^6$	$\lambda_{100} \times 10^6$	$\lambda_{111} \times 10^6$	$\lambda_{110} \times 10^6$	$\lambda_p \times 10^6$
75-15-10	+ 5	+ 9	+ 3.5	+6.2	+ 5.5	+ 5.1
85-10- 5	+16	- 8	+10.6	-5.6	- 1.5	+ 0.9
80-10-10	+29	+14	+19.4	+9.5	+11.2	+13.5
80-15- 5	+26	- 7	+17.5	-4.9	+ 0.7	+ 4.0



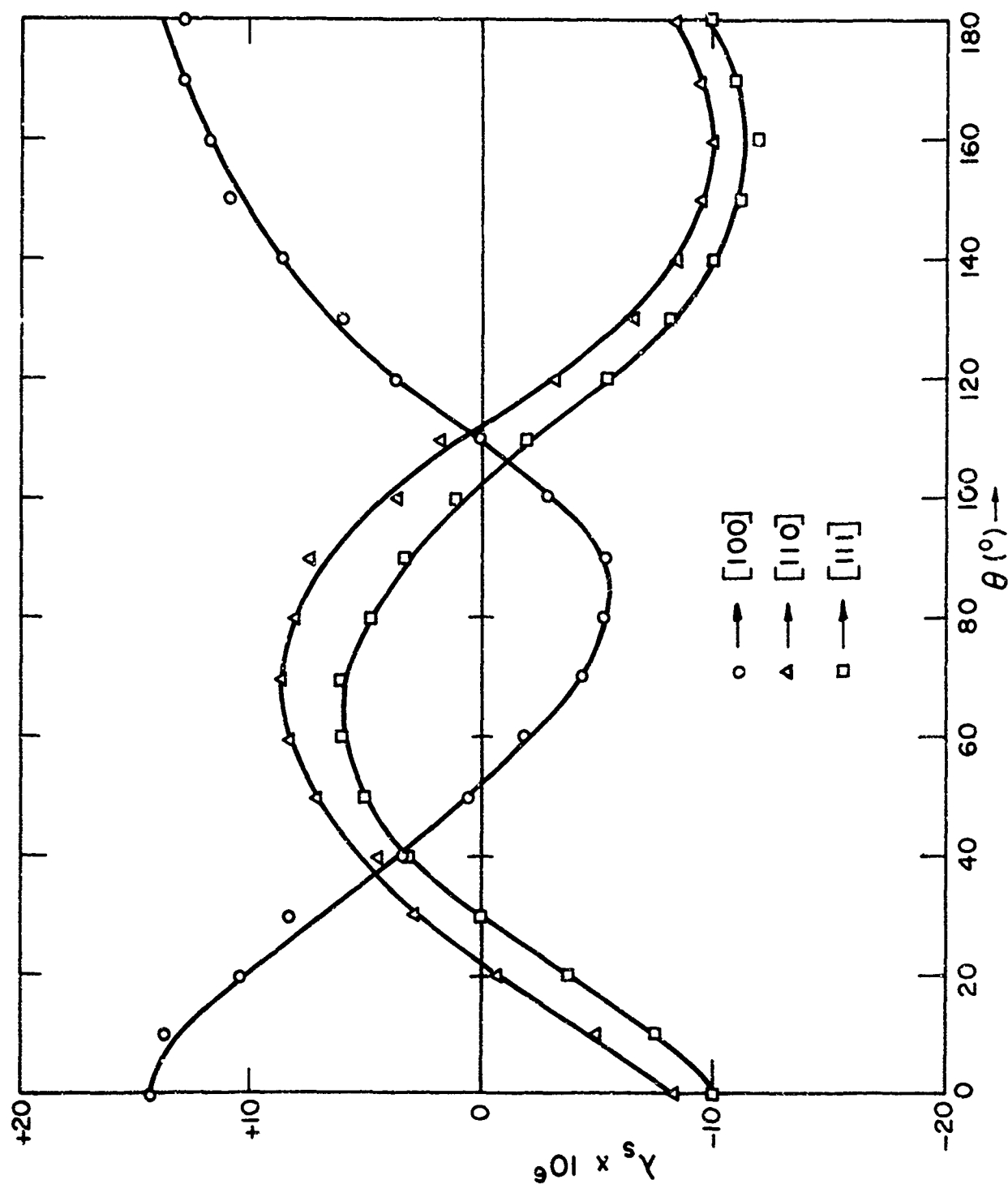


Figure 3.3 Saturation Magnetostriction Measured in the [100], [110], and [111] Directions as a Function of Angle  $\theta$  for the 75Fe-15Co-10Al Alloy

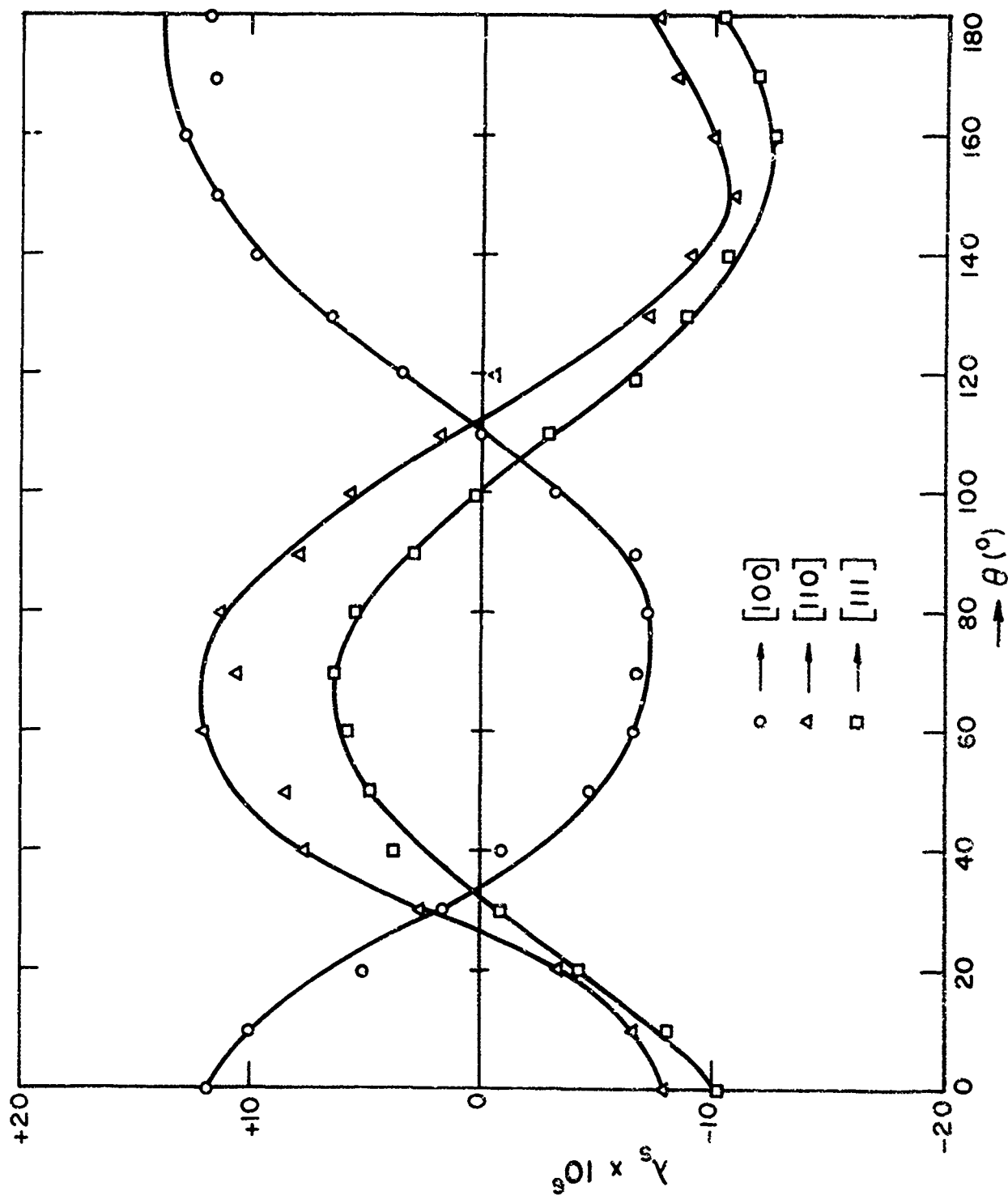


Figure 3.4 Saturation Magnetostriction Measured in the [100], [110], and [111] Directions as a Function of Angle  $\theta$  for the 85Fe-10Co-5Al alloy

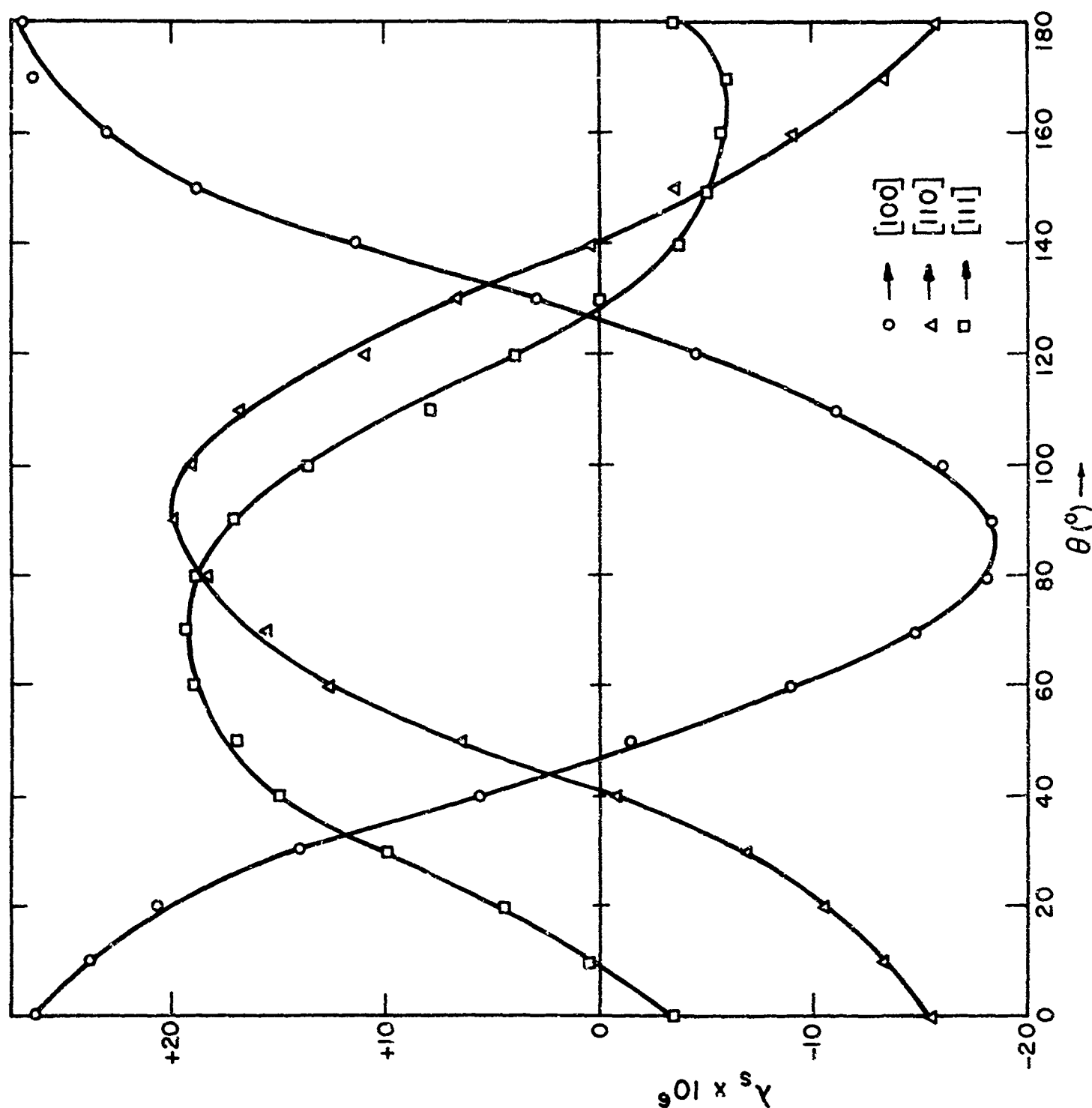


Figure 3.5 Saturation Magnetostriction Measured in the [100], [110], and [111] Directions as a Function of Angle  $\theta$  for the 80Fe-10Co-10Al Alloy

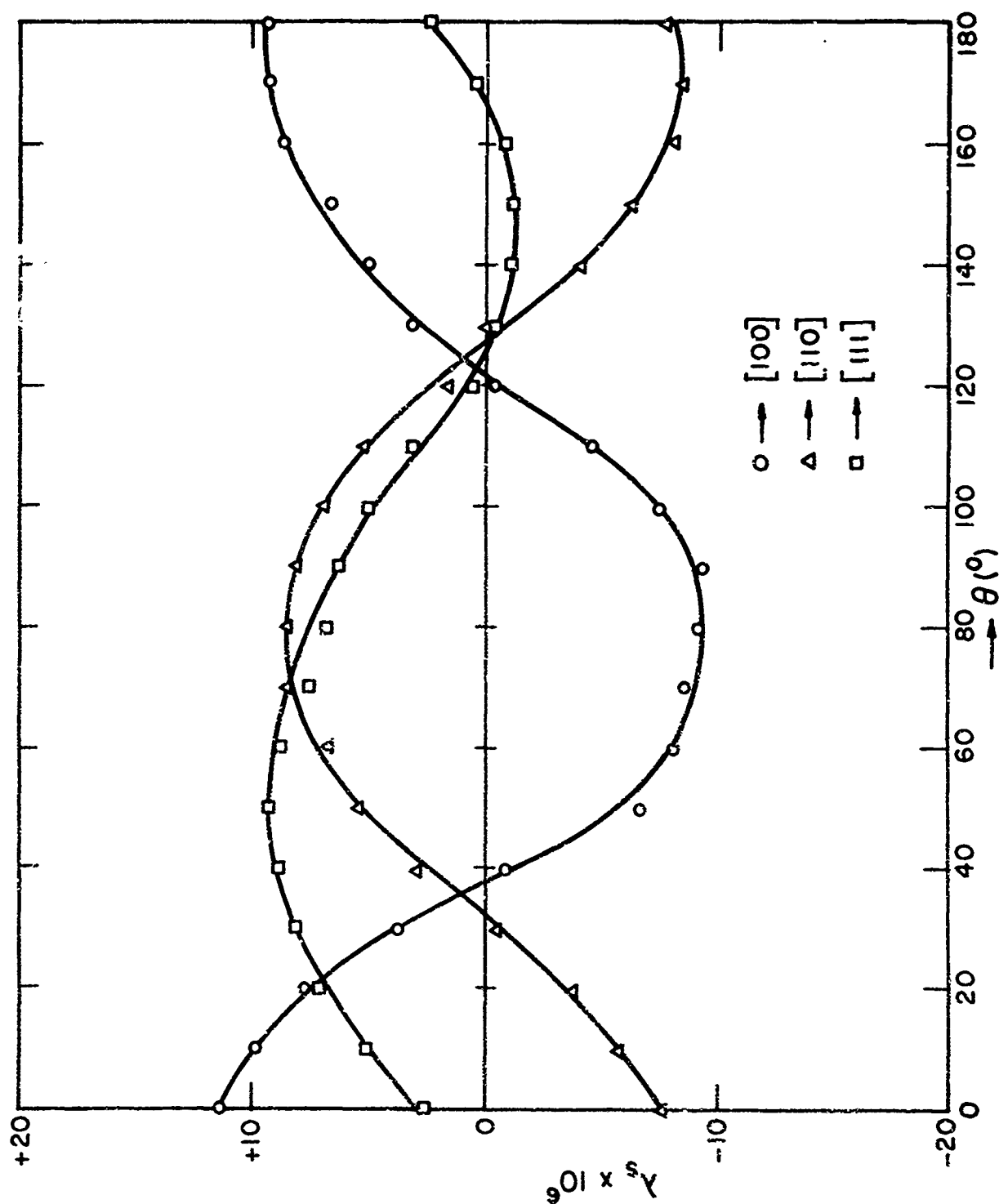


Figure 3.6 Saturation Magnetostriction Measured in the [100], [110], and [111] Directions as a Function of Angle  $\theta$  for the 80Fe-15Co-5Al Alloy

$$h_1(\text{cor}) = -1/3 \mu M_s^2 (S_{11} - S_{12})$$

$$h_2(\text{cor}) = -1/6 \mu M_s^2 S_{44}$$

where

$$\mu = (3\pi/2\epsilon^2) [(1-\epsilon^2)(3+2\epsilon^2) - (3/\epsilon)(1-\epsilon^2)^{1/2} \sin^{-1}\epsilon]$$

$$a = b = c/(1-\epsilon^2)^{1/2}$$

In these expressions,  $M_s$  is the saturation magnetization, the values of  $S$  are the various elastic constants which were taken to be those of iron,  $a$ ,  $b$ , and  $c$  are the axes of the disk, and  $\epsilon$  is the eccentricity. This correction for the so-called form effect was found to be small for these alloys and was not applied.

### 3.4 Magnetization Studies

The vibrating sample magnetometer yielded total sample moment in emu's vs. external applied magnetic field data for magnetization in the [100], [111], and [110] directions. This raw data was processed by a computer and converted to magnetization (magnetic per unit volume) vs. internal magnetic field information. This information was plotted and the area between the magnetization curves and the ordinate axis determined. This area is proportioned to the energy stored in the crystal during magnetization:

$$W = \int_0^{M_s} H dM$$

Where  $W$  is the energy stored,  $M_s$  is the saturation magnetization,  $H$  is the internal field and  $dM$  is a magnetization

increment. With this information the various magnetic anisotropy constants were determined from [10]:

$$K_0 = W_{100}$$

$$K_1 = 4(W_{110} - W_{100})$$

$$K_2 = 27(W_{111} - W_{100}) - 36(W_{110} - W_{100})$$

Where the K's are the various principle anisotropy constants and the W's are the energies required for magnetization in the specific direction, Table 3.3 lists the values of  $K_1$  obtained for the alloys studied in addition to the saturation magnetization values obtained.

Table 3.3

Saturation magnetization and anisotropy of several crystals

Composition wt.% Fe-Co-Al	Saturation magnetization, $M_s$ (emu/cc at 20°C) <sup>s</sup>	Anisotropy constant, $K_1$ (ergs/cc)
75-15-10	1090	79,000
85-10- 5	1400	2,000
80-10-10	1340	282,000
80-15- 5	1330	39,000

## CONCLUSIONS

1. The saturation magnetostriction observed in Fe rich Fe-Al and Fe-Co alloys is not a simple additive property that is enhanced by formation of the Fe-Co-Al alloys. In general, just the opposite appears to be true in that the saturation magnetostriction values observed for the Fe-Co-Al alloys studied are many times smaller than those observed in the binary alloys alone.

2. The magnetic anisotropy of Fe-Co-Al alloys can be controlled over a very wide range of values by composition adjustments.

3. It is observed that for the alloys studied a strong correlation between unit cell volume,  $K_1$ , and  $\lambda_p$  exists. The 80Fe-10Co-10Al alloy has the largest cell size, largest value of  $K_1$  and the largest value of  $\lambda_p$ . The 85Fe-10Co-5Al alloy is at the other end of the scale while the other alloys occupy predictable positions in between.

## BIBLIOGRAPHY

1. R. M. Bozorth, Ferromagnetism (Van Nostrand, New York, 1951), Chapt. 13.
2. C. Kittel, "Physical Theory of Ferromagnetic Domains", Review of Modern Physics, 21, pp. 541-583 (1949).
3. E. W. Lee, "Magnetostriiction and Magnetomechanical Effects", Reports on Progress in Physics, 18, pp. 184-229 (1955).
4. C. M. van der Burgt and A. L. Stuijts, "Development in Ferrite Ceramics with Strong Piezo agnetic Coupling", Ultrasonics, 1, 199 (1963).
5. C. A. Clark, "Improved Nickel-Base Alloys for Magnetostrictive Transducers", J. Acoust. Soc. Am., 33, 930 (1961).
6. W. S. Cramer and P. L. Smith, "Piezoceramics for Underwater Sound Transducers", J. Underwater Acoustics (USN), 15, 199 (1965).
7. R. C. Hall, "Magnetostriiction of Aluminum-Iron Single Crystals in the Region of 6 to 30 Atomic Percent", J. Appl. Phys., 28, 707 (1957).
8. R. C. Hall, "Single Crystal Anisotropy and Magnetostriction Constants of Several Ferromagnetic Materials Including Alloys of NiFe, SiFe, AlFe, CoNi and CoFe", J. Appl. Phys., 30, 816 (1959).
9. W. J. Carr and R. Smoluchowski, "The Magnetostriiction of Single Crystals of Iron-Silicon Alloys", Phys. Rev., 83, 1236 (1951).
10. F. Brailsford, Physical Principles of Magnetism (Van Nostrand, New York, 1966) p. 137.



Unclassified

Security Classification

DOCUMENT CONTROL DATA - R & D		
(Security classification of title, body of abstract and indexing annotation must be entered when the overall report is classified)		
1. ORIGINATING ACTIVITY (Corporate author) College of Engineering University of Notre Dame Notre Dame, Indiana		2a. REPORT SECURITY CLASSIFICATION Unclassified
		2b. GROUP
3. REPORT TITLE  Magnetostriction and Magnetic Anisotropy in Some Iron Rich Iron-Cobalt-Aluminum Alloys		
4. DESCRIPTIVE NOTES (Type of report and, inclusive dates) Technical Report		
5. AUTHOR(S) (First name, middle initial, last name) Michael E. Kuruzar, Mukund Phadke, and Albert E. Miller		
6. REPORT DATE February 1970	7a. TOTAL NO. OF PAGES 35	7b. NO. OF REFS 10
8a. CONTRACT OR GRANT NO. ONR-N00014-68-A-0152	9a. ORIGINATOR'S REPORT NUMBER(S) THEMIS-UND-70-6	
b. PROJECT NO.		
c. In-House Account No. UND-99850	9b. OTHER REPORT NO(S) (Any other numbers that may be assigned this report)	
d.		
10. DISTRIBUTION STATEMENT  Document cleared for public release and sale: Its distribution is unlimited.		
11. SUPPLEMENTARY NOTES		12. SPONSORING MILITARY ACTIVITY Department of Navy Office of Naval Research
13. ABSTRACT  ABSTRACT  The magnetic anisotropy and magnetostriction of single crystals and the magnetostriction of some polycrystalline specimens of several Fe rich Fe-Co-Al alloys has been experi- mentally determined. Specialized apparatus and procedures for alloy preparation, single crystal growth, crystal cutting, crystal orientation, magnetization and magnetostriction studies have been developed.  The first anisotropy constants, $K_1$ , for 75Fe-15Co-10Al (wt.%), 85Fe-1Co-5Al, 80Fe-10Co-10Al and 80Fe-15Co-5Al alloys were found to be 79,000, 2,000, 282,000, and 39,000 (ergs/cc), respectively; the $\lambda_{100}$ values were found to be $+3.5 \times 10^{-6}$ , $+10.6 \times 10^{-6}$ , $+19.4 \times 10^{-6}$ , and $+17.5 \times 10^{-6}$ , respectively; and the $\lambda_{111}$ values were found to be $+6.2 \times 10^{-6}$ , $-5.6 \times 10^{-6}$ , $+9.5 \times 10^{-6}$ , and $-4.9 \times 10^{-6}$ , respectively.		

DD FORM 1473 (PAGE 1)  
1 NOV 65

S/N 0101-807-6811

Unclassified

Security Classification

A-21409

Unclassified

Security Classification

KEY WORDS	LINK A		LINK B		LINK C	
	ROLE	WT	ROLE	WT	ROLE	WT
Magnetostriction						
Magnetization						
Magnetic Anisotropy						
Iron-Cobalt-Aluminum Alloys						

DD FORM 1475 (BACK)

STANDARD 2-1

Security Classification

A-51-01